# BILINEAR REPRESENTATIONS OF STRESS-STRAIN BEHAVIOR OF TYPES 304 AND 316 STAINLESS STEEL CYCLICLY DEFORMED AT 800-1200° F*

C. F. CHENG, C. Y. CHENG
*Materials Science Division,*
*Argonne National Laboratory, Argonne, Illinois 60439, U.S.A.*

## SUMMARY

Creep is significantly affected by temperature and loading conditions; thus, the design rules for nuclear components in Section III of the ASME Boiler and Pressure Vessel Code and ASME Code Case 1331 require inelastic analysis be performed to show that the levels of stress and strain are acceptable under given criteria. Generally, this requires a combined time-dependent creep analysis and time-independent elastic-plastic analysis in which creep and elastic-plastic behaviors are simultaneously considered. Such a combination of analyses is capable of predicting stresses, total strains accumulated, and deformations as functions of time for any random load and temperature history.

In the case of elastic-plastic analyses of Fast Flux Test Facility (FFTF) components, the tentative RDT Standard F9-1 recommends that the bilinear stress-strain relationship and the classical kinematic hardening model be used with the von Mises or the Tresca yield criterion and the associated flow rule of von Mises. This paper presents the bilinear representations of the elastic-plastic strain-hardening behavior of Types 304 and 316 stainless steel under cyclic loading conditions. The data were obtained from fully reversed, axially strain controlled low-cycle fatigue tests in air at 800-1200°F, and at $4\times10^{-3}-4\times10^{-6}$ $\sec^{-1}$ strain rate. The effects of maximum strain, temperature, heat treatment, and tension hold time on bilinear hardening functions $\varkappa$ (a measure of yield surface) and coefficients C (as related to von Mises flow law) were evaluated. These hardening coefficients and functions are discussed in relation to the work hardening that accompanies cyclic deformation.

Based on the limited low-cycle fatigue data, the conclusions are as follows:

(1) With or without tension hold time, the hardening functions $\varkappa_0$, $\varkappa_1$, and $\varkappa_s$ (subscripts 0,1 and $s$ denote monotonic and cyclic at 10th cycle and saturated stress cycle, respectively) increase with $\varepsilon_{max}$ ($\Delta\varepsilon_t/2$), and all three hardening functions converge at $\sim$0.25% $\varepsilon_{max}$.
(2) No discernible temperature trend was observed in tests without tension hold times for the cyclic hardening functions $\varkappa_1$ and $\varkappa_s$. Only the monotonic hardening function $\varkappa_0$ increases as the temperature decreases at the same $\varepsilon_{max}$.
(3) Values of $\varkappa_1$ and $\varkappa_s$ for the annealed condition are either equal to or greater than the annealed-and-aged condition in tests without tension hold time.
(4) The family of tension-hold time curves also shows $\varkappa_s$ decreases as $\varepsilon_{max}$ decreases, and they converge at $\sim$0.25% $\varepsilon_{max}$.
(5) The bilinear hardening coefficient $C$ (calculated from monotonic tensile data) decreases as $\varepsilon_{max}$ increases. Above 0.5% $\varepsilon_{max}$, the deviation of $C$ from the arithmetic average over a temperature range from 800 to 1200°F appears insignificant.

* Work performed under the auspices of the U.S. Atomic Energy Commission.

## 1. Introduction

Inelastic analyses are often required under provisions of the ASME Boiler and Pressure Vessel Code Section III and the ASME Code Case 1331. These documents specify the method of incorporating the values of stresses and strains that are determined by inelastic analyses into the evaluation of nuclear components and give criteria for determining acceptable levels of these stresses and strains. They do not, however, specify the techniques or methods to be used in predicting the stresses and strains. Accordingly, recommendations for analytical methods and constitutive equations have been prepared by Oak Ridge National Laboratory (ORNL) for the inelastic analyses of Fast Flux Test Facility (FFTF) components [1].

In the FFTF design document [2], ORNL recommended that mathematical descriptions for creep and plasticity be formulated independently. For elastic-plastic behavior, ORNL recommended that Prager's classical kinematic hardening model be used with the von Mises flow law and either the von Mises or Tresca yield criteria. Specific requirements for the determination of the plastic-strain and creep-strain components have been proposed by ORNL in the tentative RDT Standard F9-1 [3]. The present report deals only with the bilinear representations of the elastic-plastic strain-hardening behavior of Types 304 and 316 stainless steel under cyclic loading conditions.

At present, no material properties data are available for bilinear representations of the cyclic stress-strain behavior of Types 304 and 316 stainless steel in the Liquid Metal Fast Breeder Reactor (LMFBR) Materials Handbook [4]. Accordingly, the Hanford Engineering Development Laboratory (HEDL) requested Research Development and Technology (RDT) to supply the bilinear representation data through RDT-sponsored low-cycle high-temperature fatigue programs at Argonne National Laboratory (ANL), Aerojet Nuclear Corporation (ANC), and Battelle Memorial Institute (BMI) [5]. ANL was assigned the responsibility of gathering, evaluating, and supplying this data to HEDL for incorporation into the LMFBR Materials Handbook [6].

## 2. Method of Evaluation

Constants for bilinear representation of the stress-strain curves were determined in accordance with ref. [3]. The values of the hardening coefficient C, the elastic slope $E_e$, and the monotonic hardening function $\kappa_o$ were obtained from the true stress-true strain relationship in the LMFBR Materials Handbook (pages 22a and b for Type 304 stainless steel and pages 8a and b for Type 316) [4]. Using the graphical construction illustrated in Fig. 1a, the slope $E_m$ of the elastic-plastic line was obtained by connecting N (the stress at maximum strain $\epsilon_{max}$) to M (the stress at strain $\epsilon_{max}/2$). Similarly, the slope $E_p$ of the stress-plastic strain line was determined by joining N' (the stress equal to N at plastic strain D) to S' (the stress equal to the yield point S at zero plastic strain). Location of D at the strain axis was determined by making DN parallel to OS.

Using the constructed bilinear curve, the values of C and $\kappa_o$ were computed as follows:

$$C = \frac{2}{3} E_p \quad \text{and} \quad \kappa_o = \frac{\sigma_o^2}{3} ,$$

where $\sigma_o$ is the yield point at the intersection S of the elastic line OS and elastic-plastic line NMS. The slope $E_m$ of the elastic-plastic line is

$$1.5\ E_e C/(E_e + 1.5\ C),$$

where $\varepsilon_{max}/\sigma' = \varepsilon_e/\sigma' + \varepsilon_p/\sigma'$, or $1/E_m = 1/E_e + 1/E_p = 1/E_e + 1/(1.5\ C)$.

Therefore, $$E_m = 1.5\ E_e C/(E_e + 1.5\ C).$$

Values of bilinear cyclic hardening functions were also determined for the tenth cycle of loading ($\kappa_1$) and for the saturated-stress cycle ($\kappa_s$) by constructing a bilinear curve with the same slope $E_m$ as the monotonic curve. The location of this curve was constructed so that the areas above and below the actual stress-strain hysteresis loop in either the tensile or compressive stress region were approximately equal for cycles without hold times (Fig. 1b) and for cycles with tension hold time (Fig. 1c). The following equation was then used to calculate $\kappa_1$ and $\kappa_s$:

$$\kappa_1 = \frac{\sigma_1^2}{12} \text{ and } \kappa_s = \frac{\sigma_s^2}{12},$$

where $\sigma_1$ and $\sigma_s$ are defined as in Fig. 1.

3. Results

The hardening functions for the bilinear representation of the cyclic hardened stress-strain hysteresis loops for Types 304 and 316 stainless steel in low-cycle fatigue tests without and with tension hold time are summarized in Tables I and II, respectively. The stress range ($\Delta\sigma$) at $N_f/2$, the initial saturated stress cycle ($N_s$), the cycles to failure ($N_f$), tension hold time ($t_H$), and equivalent frequency ($\gamma$) are also included in these tables. The equivalent frequency $\gamma$ is obtained from the equation $\gamma \equiv \left(t_H + \frac{1}{\gamma'}\right)^{-1}$, where $\gamma'$ is the ramp frequency.

All tests were conducted at an axially controlled strain rate of $4 \times 10^{-3}$ to $4 \times 10^{-6}$ $sec^{-1}$, at total strain ranges of approximately 1/2 to 4%, and at temperatures between 800 and 1200°F. The bulk of the data is at a strain rate of $4 \times 10^{-3}$ $sec^{-1}$ between 1/2 and 3% total strain range and between 1050 and 1200°F. The data were collected from tests performed at ANL, ANC, and BMI; the heat analyses have been previously reported [7].

The typical stress-strain hysteresis loops for annealed and aged Type 304 stainless steel in low-cycle fatigue tests at 2% $\Delta\varepsilon_t$ and 1100°F with and without tension hold time are shown in the hysteresis loops after saturated stress cycle 14 in Fig. 2a and cycle 88 in Fig. 2b. Generally, stress saturation is attained early in fatigue life and any hysteresis loop after stress saturation can be used to determine $\kappa_s$.

The hardening functions $\kappa_o$, $\kappa_1$, and $\kappa_s$ for Types 304 and 316 stainless steel in Table I are plotted in relation to maximum strain ($\varepsilon_{max} = \Delta\varepsilon_t/2$, where $\Delta\varepsilon_t$ is the total axial strain range) in Figs. 3-4 for low-cycle fatigue. Figures 3a and 3b show the square root of $\kappa_o$, $\kappa_1$, and $\kappa_s$ versus $\varepsilon_{max}$ from 800 to 1200°F for Type 304 stainless steel, whereas Figs. 4a, b, and c are for Type 316 stainless steel. The square root of the bilinear function is used because $\kappa^{1/2}$ is directly proportional to the applied stress. In the case of low-cycle fatigue tests with tension hold time, the hardening functions for Types 304 and 316 stainless steel in Table II are plotted in relation to an equivalent frequency $\gamma$. Figure 3c shows the relationship of $\kappa_s^{1/2}$ versus $\gamma$ at 1, 1/2, and 1/4% $\varepsilon_{max}$ from 1000 to 1200°F.

The bilinear hardening coefficient (C) for Types 304 and 316 stainless steel at 800-1200°F in Table III are plotted in relation to maximum strain ($\varepsilon_{max}$) in Fig. 3d. The data were calculated from the true stress-true strain relationship in the LMFBR Materials Handbook [4].

4. Discussion

The bilinear representations of the stress-strain behavior of Types 304 and 316 stainless steel cyclicly deformed at 800-1200°F are discussed below in relation to the influences of maximum strain, temperature, heat treatment, tension hold time, and strain rate.

4.1 Maximum Strain

For tests with and without tension hold time, the hardening functions decrease with a decrease in maximum strain at a given temperature (Figs. 3a and b and 4a, b, c, and d). This is characteristic of cyclic-hardening material such as Types 304 and 316. Also, as expected at 1% $\varepsilon_{max}$, the value for the cyclic hardening function $\kappa_s$ at a saturated stress cycle is larger than the corresponding $\kappa_1$ at the tenth cycle, and both are much greater than the monotonic hardening function $\kappa_o$. However, all $\kappa$ curves converge at $\sim$ 0.25% $\varepsilon_{max}$.

In the case of the bilinear hardening coefficient C, Fig. 3c shows that C, as expected, decreases as $\varepsilon_{max}$ increases for temperatures from 800 to 1200°F (Table III). The deviation from the average value decreases with an increase in $\varepsilon_{max}$. This is attributed to the shape of the true stress-true strain curves at these temperatures. Apparently, above 1/2% $\varepsilon_{max}$, C is essentially independent of temperature.

4.2 Temperature

Each curve in Figs. 3a and b and 4a, b, c, and d for cyclic hardening functions $\kappa_1$ and $\kappa_s$ applies to a specific material and testing condition. Accordingly, a family of these curves, which were generated from specimens with the same heat treatment, without tension hold time, and with test temperatures that ranged from 800 to 1200°F, was plotted in one figure to evaluate the temperature effect. These curves are not reproduced here, because no discernible temperature trend could be detected. Only the monotonic hardening function $\kappa_o$ increases as the temperature decreases.

4.3 Heat Treatment

At a test temperature of 1050°F and without tension hold time, Fig. 3a shows no significant difference in $\kappa_s$ and $\kappa_1$ between the annealed and the annealed and aged (1000 hr at test temperature) conditions for type 304 stainless steel. However, at 1100°F (Fig. 3b), the same observation is true for $\kappa_s$, but different $\kappa_1$ curves were obtained for the annealed and the annealed and aged conditions. This can readily be understood in terms of carbide precipitation due to heat treatment before testing and subsequent cyclic deformation. At the start of the test, the difference in carbide precipitation between the annealed and the annealed and aged conditions is smaller at 1050°F than at 1100°F. As the specimen approaches saturated stress in cycling, the difference disappears because of the enhancement of carbide precipitation by cyclic deformation [7]. In the case of Type 316 stainless steel, both $\kappa_s$ and $\kappa_1$ have different curves for the annealed and the annealed and aged conditions at 1200°F (Fig. 4a) and 1050°F (Fig. 4b).

4.4 Tension Hold Time

Figure 3c shows that $\kappa_s$ decreases as the tension hold time increases, indicating a recovery effect. Note that the logarithmic relationship of $\gamma$ versus $\kappa_s^{1/2}$ is linear, and its slope decreases as $\varepsilon_{max}$ decreases. At 1/4% $\varepsilon_{max}$, the slope approaches zero. A family of tension-hold-time curves of $\kappa_s^{1/2}$ versus $\varepsilon_{max}$ is plotted in Fig. 3b for Type 304 stainless steel at 1100°F and in Figs. 4a and 4c for Type 316 at 1100 and 1200°F, respectively. Note that these tension-hold-time curves converge at low $\varepsilon_{max}$. The 100-hr tension-hold-time curve was extrapolated from Fig. 3c. Extrapolation beyond 100 hr may not be realistic because of possible saturation effects.

4.5 Strain Rate

A few slower strain rate tests (Table II) were also conducted to investigate the effect of strain rate and to compare its influence on fatigue life with tension hold time. As shown in Fig. 3c, it appears that no significant difference in the $\kappa_s$ values occurred under these two loading conditions. However, in previous study [8], it was found that equivalent hold time in compression only or symmetrical hold time does have longer fatigue life than tension hold time. Further study is needed to clarify the frequency effect.

5. Conclusions and Recommendations

Based on low-cycle fatigue data available for Types 304 and 316 stainless steel in Tables I and II, most of which was at an axially controlled strain rate of $4 \times 10^{-3}$ $sec^{-1}$ and test temperatures from 800 to 1200°F, the conclusions and recommendations can be summarized as follows:

(1) With or without tension hold time, the hardening functions $\kappa_o$, $\kappa_1$, and $\kappa_s$ (subscripts o, 1, and s denote monotonic, cyclic at the tenth cycle, and cyclic at the saturated stress cycle, respectively) increase with $\varepsilon_{max}$ $(\Delta\varepsilon_t/2)$, and all three hardening functions converge at $\sim$ 0.25% $\varepsilon_{max}$.

(2) No discernible temperature trend was observed in tests without tension hold times for the cyclic hardening functions $\kappa_1$ and $\kappa_s$. Only the monotonic hardening function $\kappa_o$ increases as the temperature decreases at the constant $\varepsilon_{max}$.

(3) Values of $\kappa_1$ and $\kappa_s$ for the annealed condition are either equal to or greater than the annealed and aged condition in tests without tension hold time.

(4) The family of tension-hold-time curves also shows that $\kappa_s$ decreases as $\varepsilon_{max}$ decreases, and they converge at $\sim$ 0.25% $\varepsilon_{max}$.

(5) In Type 304 stainless steel at 1100°F, $\kappa_s$ decreases as the equivalent frequency ($\gamma$) decreases, irrespective of imposed strain rate or tension hold time.

(6) The bilinear hardening coefficient C (calculated from monotonic tensile data) decreases as $\varepsilon_{max}$ increases. Above 0.5% $\varepsilon_{max}$, the deviation of C from the arithmetic average over a temperature range from 800 to 1200°F appears insignificant.

(7) At 0.25% $\varepsilon_{max}$ or below and temperatures from 800 to 1200°F, $\kappa_s^{1/2}$ values of 1.0 and $1.5 \times 10^4$ psi (with or without tension hold time) are recommended for Types 304 and 316 stainless steel, respectively. At 0.5% $\varepsilon_{max}$, the $\kappa_s^{1/2}$ values of 1.5 and $2.0 \times 10^4$ psi are recommended for tension hold times of 100 hr or more. For all other conditions, refer to the $\kappa_s^{1/2}$ curves provided in the present report.

Acknowledgments

The author wishes to acknowledge the cooperation of Dr. C. R. Brinkman of Aerojet Nuclear Corporation, Idaho Falls, Idaho and Dr. C. E. Jaske of Battelle Memorial Institute, Columbus Laboratories, Columbus, Ohio in furnishing their low-cycle fatigue data and calculating the corresponding bilinear hardening functions. Thanks are extended to W. J. Burke and C. F. Peterson for their assistance in obtaining the data from tests conducted at Argonne National Laboratory. Also, special thanks are extended to Dr. R. W. Weeks for reviewing the manuscript.

References

[1] PUGH, C. E., CORUM, J. M., LIU, K. C., GREENSTREET, W. L., Currently Recommended Constitutive Equations for Inelastic Design Analysis of FFTF Components, ORNL-TM-3602 (Sept. 1972).

[2] SNOW, A. L., private communication (1971).

[3] RDT Standard F9-1 (Jan. 20, 1972, tentative).

[4] Hanford Engineering Development Laboratory, private communication (1971).

[5] EVANS, E. H., private communication (1972).

[6] SINCLAIR, E. E., private communication (1972).

[7] CHENG, C. F., CHENG, C. Y., DIERCKS, D. R., WEEKS, R. W., "Low-Cycle Fatigue Behavior of Types 304 and 316 Stainless Steel at LMFBR Operating Temperatures", ASTM Sym. on Fatigue at Elevated Temperatures, Storrs, Conn., June 1972 (to be published).

[8] CHENG, C. Y., DIERCKS, D. R., "Effects of Hold Time on Low-Cycle Fatigue Behavior of AISI Type 304 Stainless Steel at 593°C", Met. Trans. 4, 615-617 (1973).

TABLE 1. Bilinear Hardening Functions for Low-cycle Fatigue without Tension Hold Time[a]

| Temperature, °F | Testing Laboratory | Specimen Number | $\Delta\varepsilon_t$, % | $\Delta\varepsilon_p$, % | $\Delta\sigma_t$, ksi | $N_c$, Cycles | $N_f$, Cycles | $\kappa_0^{1/3}$, psi x $10^{-4}$ | $\kappa_1^{1/3}$, psi x $10^{-4}$ | $\kappa_s^{1/3}$, psi x $10^{-4}$ |
|---|---|---|---|---|---|---|---|---|---|---|
| | | | | Type 304 Stainless Steel[b] | | | | | | |
| Annealed | | | | | | | | | | |
| 1200 | BMI | SS-18 | 2.73 | 2.30 | 98 | - | 385 | 1.03 | 2.40 | 2.50 |
| | BMI | SS-15 | 1.89 | 1.50 | 103 | - | 744 | 1.01 | 2.18 | 2.30 |
| | ANL | 3A-2 | 0.84 | 0.60 | 51 | 135 | 3504 | 0.91 | 1.35 | 1.65 |
| | BMI | SS-5 | 0.47 | 0.25 | 53 | - | 1882 | 0.84 | 0.97 | 1.11 |
| 1100 | ANL | - | 10.0 | 9.45 | (118)[A] | - | - | 1.27 | (3.06)[A] | (3.15)[A] |
| | ANL | T101 | 4.05 | 3.45 | 112 | 17 | 158 | 1.15 | 2.91 | 2.99 |
| | ANL | T21 | 3.13 | 2.65 | 106 | 31 | 177 | 1.10 | 2.67 | 2.76 |
| | ANL | AA-2 | 2.02 | 1.69 | 92 | 86 | 737 | 1.04 | 2.07 | 2.24 |
| | ANL | 8A-8 | 1.99 | 1.57 | 92 | 43 | 806 | 1.04 | 2.12 | 2.36 |
| | ANC | A-31 | 1.0 | 0.63 | 78 | - | 2737 | 0.96 | 1.55 | 1.78 |
| | ANL | AA-11 | 0.76 | 0.45 | 65 | 235 | 4835 | 0.93 | - | 1.48 |
| | ANC | A-200 | 0.52 | 0.28 | 51 | - | 115 | 0.88 | 0.85 | 1.08 |
| | ANL | AA-12 | 0.36 | 0.16 | 44 | - | 52343 | 0.86 | - | 0.92 |
| 1050 | ANL | 8A-7 | 2.01 | 1.67 | 97 | 89 | 996 | 1.06 | 2.05 | 2.42 |
| | ANL | 8A-1 | 1.00 | 0.63 | 83 | 123 | 2811 | 0.98 | 1.39 | 1.72 |
| | ANL | 8A-6 | 0.50 | 0.26 | 53 | 431 | 17273 | 0.92 | 0.90 | 1.11 |
| 1000 | BMI | SS-1 | 2.90 | 0.40 | 108 | - | 390 | 1.15 | 2.44 | 2.66 |
| | BMI | SS-12 | 2.04 | 1.65 | 104 | - | 737 | 1.10 | 2.16 | 2.48 |
| | ANL | 3A-11 | 1.02 | 0.53 | 61 | 223 | 3931 | 1.02 | 1.14 | 1.51 |
| | BMI | SS-21 | 0.63 | 0.36 | 59 | - | 10282 | 0.96 | - | 0.80 |
| Annealed and Aged (1000 hr at Test Temperature) | | | | | | | | | | |
| 1100 | ANL | AA-4 | 2.02 | 1.60 | 93 | 57 | 935 | 1.04 | 2.07 | 2.30 |
| | ANL | T-31 | 1.50 | 1.08 | 86 | 172 | 1625 | 1.01 | 1.53 | 2.15 |
| | ANL | AA-7 | 1.01 | 0.69 | 71 | 205 | 398 | 0.96 | 1.29 | 1.67 |
| | ANL | AA-22 | 0.75 | 0.43 | 62 | 449 | 7002 | 0.93 | 0.92 | 1.31 |
| | ANL | AA-8 | 0.50 | 0.26 | 45 | - | 30498 | 0.88 | 0.67 | 1.15 |
| 1050 | ANL | 5A-3 | 2.01 | 1.58 | 96 | 60 | 1070 | 1.06 | 2.12 | 2.25 |
| | ANL | 5A-1 | 1.02 | 0.69 | 75 | 323 | 4326 | 0.98 | 1.38 | 1.69 |
| | | | | Type 316 Stainless Steel[c] | | | | | | |
| Annealed | | | | | | | | | | |
| 1200 | BMI | 17 | 2.04 | 1.54 | 104 | - | 354 | 1.12 | 2.42 | 2.58 |
| | ANL | GR1-1 | 1.93 | 1.49 | 113 | 87 | 459 | 1.12 | 2.55 | 2.68 |
| | BMI | 18 | 1.03 | 0.62 | 92 | - | 1089 | 1.05 | 2.00 | 2.19 |
| | ANL | GR1-2 | 0.92 | 0.54 | 85 | 102 | 1721 | 1.05 | 1.52 | 2.11 |
| | BMI | 20 | 0.79 | 0.43 | 79 | 170 | 2846 | 1.04 | 1.45 | 1.70 |
| | BMI | 19 | 0.49 | 0.20 | 63 | - | 10001 | 0.99 | 1.20 | 1.49 |
| 1100 | ANL | - | 10.0 | 9.28 | (153)[B] | - | - | 1.44 | (4.02)[B] | (4.16)[B] |
| | ANL | GR2-7 | 3.93 | 3.30 | 142 | 17 | 113 | 1.26 | 3.94 | 4.00 |
| | ANC | D-143 | 2.0 | 1.45 | 128 | - | 450 | 1.17 | 2.35 | 3.37 |
| | ANC | D-148 | 1.0 | 0.58 | 100 | - | 2040 | 1.09 | 1.37 | 2.35 |
| | ANC | D-147 | 0.5 | 0.22 | 67 | - | 24850 | 1.02 | 1.07 | 1.40 |
| 1050 | BMI | 13 | 3.08 | 2.41 | 137 | - | 130 | 1.26 | 3.17 | 3.51 |
| | ANL | GR1-8 | 1.99 | 1.42 | 112 | 78 | 564 | 1.19 | - | 3.17 |
| | BMI | 14 | 1.93 | 1.32 | 125 | - | 473 | 1.19 | 2.45 | 3.17 |
| | BMI | 15 | 1.02 | 0.57 | 96 | - | 1955 | 1.11 | 1.62 | 1.99 |
| | BMI | 16 | 0.49 | 0.20 | 66 | - | 23601 | 1.03 | - | 1.34 |
| 900 | BMI | 3 | 2.98 | 2.40 | 154 | - | 265 | 1.26 | 3.11 | 3.73 |
| | BMI | 4 | 2.02 | 1.48 | 128 | - | 897 | 1.22 | 2.44 | 2.76 |
| | BMI | 5 | 1.02 | 0.68 | 88 | - | 4026 | 1.16 | 1.51 | 1.81 |
| | BMI | 6 | 0.50 | 0.25 | 69 | - | 26938 | 1.09 | - | 1.47 |
| 800 | BMI | 8 | 2.98 | 2.39 | 154 | - | 376 | 1.33 | 3.17 | 3.32 |
| | BMI | 1 | 2.01 | 1.38 | 128 | - | 1048 | 1.26 | 2.49 | 2.73 |
| | BMI | 2 | 1.00 | 0.69 | 79 | - | 6214 | 1.18 | 1.54 | 1.56 |
| | BMI | 7 | 0.50 | 0.25 | 67 | - | 35461 | 1.11 | - | 1.42 |
| Annealed and Aged (1000 hr at Test Temperature) | | | | | | | | | | |
| 1200 | BMI | 56 | 2.64 | 2.20 | 100 | - | 363 | 1.17 | 2.42 | 2.42 |
| | BMI | 52 | 1.86 | 1.45 | 90 | - | 709 | 1.12 | 2.20 | 2.20 |
| | BMI | 50 | 0.92 | 0.58 | 72 | - | 2372 | 1.05 | 1.45 | 1.57 |
| | BMI | 58 | 0.70 | 0.40 | 68 | 35 | 4726 | 1.04 | 1.42 | 1.53 |
| | BMI | 54 | 0.48 | 0.24 | 56 | - | 9536 | 0.99 | 1.14 | 1.24 |
| 1050 | BMI | 31 | 2.86 | 2.33 | 133 | - | 254 | 1.27 | 3.05 | 3.40 |
| | BMI | 30 | 1.93 | 1.39 | 120 | - | 725 | 1.19 | 2.34 | 2.84 |
| | ANL | 20-4 | 1.98 | 1.44 | 121 | 99 | 618 | 1.19 | 2.41 | 2.98 |
| | ANL | 35-5 | 1.01 | 0.61 | 101 | 236 | 4167 | 1.11 | 1.26 | 1.88 |
| | BMI | 32 | 0.69 | 0.39 | 80 | - | 3521 | 1.06 | 1.16 | 1.62 |
| | ANL | 20-2 | 0.50 | 0.21 | 127 | 26009 | 29005 | 1.03 | - | 1.56 |

a,b,c See Table II notes.

[A] Extrapolated data from 4.05% $\Delta\varepsilon_t$ (T01) Type 304; [B] Extrapolated data from 3.93% $\Delta\varepsilon_t$ (GR2-7) Type 316.

TABLE II. Bilinear Hardening Functions for Low-cycle Fatigue with Tension Hold Time[a]

| Temperature °F | Testing Laboratory | Specimen Number | $\Delta\varepsilon_t$, % | $\Delta\varepsilon_p$, % | $t_H$, min | $\gamma$, cpm x $10^{-2}$ | $N_s$, ksi | $N_s$, cycles | $N_f$, cycles | $\sigma_H$, psi x $10^{-4}$ |
|---|---|---|---|---|---|---|---|---|---|---|
| | | | | | Type 304 Stainless Steel[b] | | | | | |
| Annealed and Aged (1000 hr at 1100°C) | | | | | | | | | | |
| 1100 | ANL | AA-4 | 2.02 | 1.60 | 0 | 594 | 93 | 57 | 935 | 2.30 |
| | ANL | T-44 | 2.01 | 1.65 | 15 | 6.6 | 88 | 40 | 237 | 2.23 |
| | ANL | T-217 | 1.98 | 1.66 | 60 | 1.66 | 82 | 30 | 112 | 2.09 |
| | ANL | AA-10 | 1.00 | 0.75 | 1 | 92 | 72 | 220 | 1064 | 1.67 |
| | ANL | AA-23 | 1.00 | 0.71 | 10 | 9.9 | 65 | 165 | 636 | 1.64 |
| | ANL | T-30 | 1.01 | 0.69 | 15 | 6.6 | 65 | 205 | <666 | 1.49 |
| | ANL | AA-27 | 1.00 | 0.73 | 60 | 1.66 | 62 | 128 | 338 | 1.47 |
| | ANL | 10A-2 | 0.49 | 0.27 | 1 | 96 | 46 | 204 | 14970 | 1.05 |
| | ANL | 62-6 | 0.51 | 0.26 | 1 | 96 | 52 | 179 | ~10441 | 1.11 |
| | ANL | AA-28 | 0.50 | 0.25 | 10 | 9.96 | 50 | 1179 | 3803 | 1.11 |
| | ANL | 62-10 | 0.50 | 0.28 | 60 | 1.67 | 48 | 106 | 2067 | 1.10 |
| | ANL | 59-12 | 1.00 | 0.66 | 0 | 120[A] | 55 | 112 | 1031 | 1.69 |
| | ANL | T-216 | 2.07 | 1.58 | 0 | 5.8[B] | 86 | 88 | 244 | 2.26 |
| | ANL | T-54 | 2.01 | 1.70 | 60 | 1.62[B] | 80 | 14 | 102 | 1.90 |
| | ANL | AA-25 | 1.00 | 0.67 | 0 | 12.0[B] | 73 | 95 | 851 | 1.73 |
| | ANL | T-70 | 0.99 | 0.73 | 60 | 1.46[B] | 68 | 81 | 305 | 1.71 |
| | ANL | T-85 | 1.07 | 0.73 | 0 | 1.20[C] | 62 | 20 | 579 | 1.49 |
| | | | | | Type 316 Stainless Steel[c] | | | | | |
| Annealed | | | | | | | | | | |
| 1200 | BMI | 2A | 1.95 | 1.59 | 6 | 16.23 | 101 | 25 | 86 | 2.53 |
| | ANL | GR1-3 | 2.08 | 1.87 | 10 | 9.83 | 88 | 20 | 91 | 2.30 |
| | BMI | 26 | 1.93 | 1.60 | 60 | 1.66 | 89 | 10 | 85 | 2.29 |
| | ANL | GR2-2 | 1.02 | 0.65 | 1 | 92 | 83 | 104 | 460 | 2.04 |
| | BMI | 25 | 1.03 | 0.72 | 6 | 16.32 | 72 | 30 | 412 | 1.64 |
| | BMI | 88 | 1.00 | 0.75 | 60 | 1.66 | 66 | 25 | 220 | 1.60 |
| Annealed | | | | | | | | | | |
| 1100 | ANC | D-131 | 2.0 | 1.43 | 0.6 | 130.6 | 133 | 37 | 218 | 3.27 |
| | ANC | D-197 | 2.0 | 1.39 | 6.0 | 16.22 | 127 | 25 | 71 | 3.26 |
| | ANC | D-188 | 1.99 | 1.59 | 30 | 3.31 | 113 | 20 | 57 | 2.98 |
| | ANC | D-198 | 2.0 | 1.66 | 60 | 1.66 | 110 | 20 | 43 | 2.82 |
| | ANC | D-114 | 2.0 | 1.61 | 309.6 | 0.323 | 103 | 13 | 25 | 2.60 |
| | ANC | D-142 | 1.0 | 0.57 | 0.6 | 146.4 | 102 | 96 | 1170 | 2.27 |
| | ANC | D-164 | 1.0 | 0.59 | 6 | 16.44 | 86 | 129 | 393 | 2.13 |
| | ANC | D-184 | 1.0 | 0.58 | 6 | 16.44 | 87 | 164 | 438 | 2.08 |
| | ANC | D-145 | 0.98 | 0.58 | 30 | 3.34 | 91 | 45 | 221 | 2.12 |
| | ANC | D-173 | 1.0 | 0.67 | 600 | 0.167 | 89 | 17 | 84 | 2.10 |
| | ANC | D-141 | 0.51 | 0.17 | 0.6 | 154.6 | 68 | 1750 | 8400 | 1.47 |
| | ANC | D-177 | 0.50 | 0.16 | 6 | 16.55 | 68 | 500 | 1985 | 1.44 |
| | ANC | D-162 | 0.50 | 0.27 | 60 | 1.67 | 72 | 85 | 812 | 1.41 |

[a] $\Delta\varepsilon_t$ is total axial strain range; $\Delta\varepsilon_p$ is plastic strain range; $t_H$ is tension hold time; $\gamma$ is equivalent frequency; $\Delta\sigma$ is stress range at $N_f/2$; $N_s$ is initial saturated stress cycle; and $N_f$ is cycles to failure. All tests are at 4 x $10^{-3}$ $sec^{-1}$ ramp strain rate unless indicated.

[b] AA and T series in HT 9T2796; remainder HT 55697. [c] HT 65808.

[A] 4 x $10^{-4}$ $sec^{-1}$; [B] 4 x $10^{-5}$ $sec^{-1}$; and [C] 4 x $10^{-6}$ $sec^{-1}$ ramp strain rate.

TABLE III. Maximum Strain Versus Bilinear Hardening Coefficient

| $\varepsilon_{max}$, % | C, psi x $10^{-5}$ | | | | | |
|---|---|---|---|---|---|---|
| | 1200°F | 1100°F | 1050°F | 1000°F | 800°F | Average |
| | | | Type 304 Stainless Steel | | | |
| $\varepsilon_{max}$, % | | | | | | |
| 2.00 | 1.87 | 1.77 | 1.83 | 1.83 | 2.07 | 1.87 |
| 1.50 | 2.00 | 2.30 | 2.07 | 2.30 | 2.27 | 2.19 |
| 1.00 | 3.00 | 2.93 | 2.93 | 3.00 | 3.13 | 3.00 |
| 0.50 | 5.00 | 5.06 | 5.60 | 4.97 | 5.33 | 5.19 |
| 0.25 | 10.20 | 10.40 | 12.00 | 10.33 | 9.93 | 10.57 |
| | | | Type 316 Stainless Steel | | | |
| 2.00 | 1.87 | 2.13 | 1.87 | 1.97 | 2.10 | 1.99 |
| 1.50 | 2.33 | 2.40 | 2.33 | 2.47 | 2.20 | 2.35 |
| 1.00 | 2.97 | 3.53 | 3.27 | 3.27 | 3.80 | 3.35 |
| 0.50 | 5.33 | 5.73 | 5.87 | 5.73 | 6.30 | 5.79 |
| 0.25 | 11.67 | 10.53 | 10.87 | 11.33 | 12.73 | 11.45 |

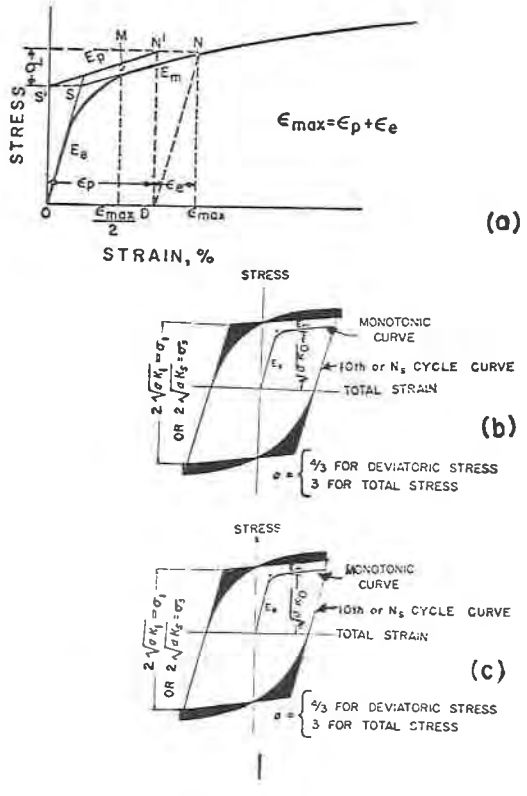


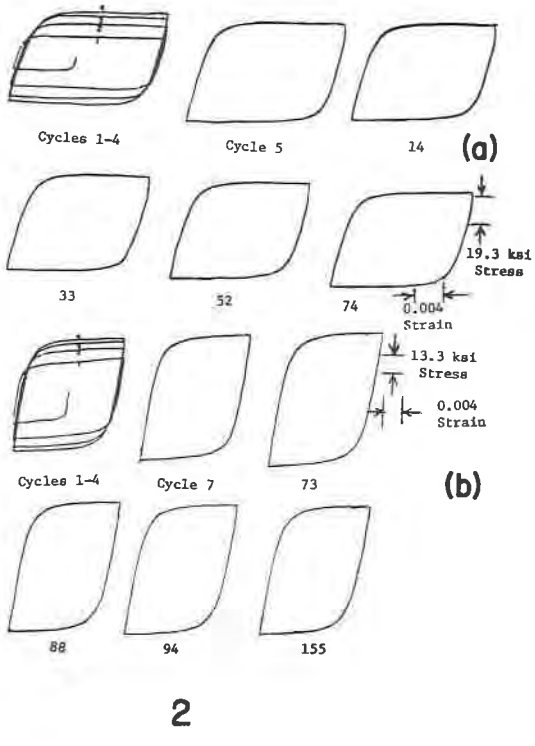


Fig. 1. Graphical construction of bilinear of representation.
Fig. 2. Stress-strain hysteresis loops of annealed and aged Type 304 — 2% $\Delta\varepsilon_t$, 1100°F, and 4 x $10^{-5}$ $sec^{-1}$ ramp strain rate. (a) 60-min tension hold time and (b) without tension hold time.

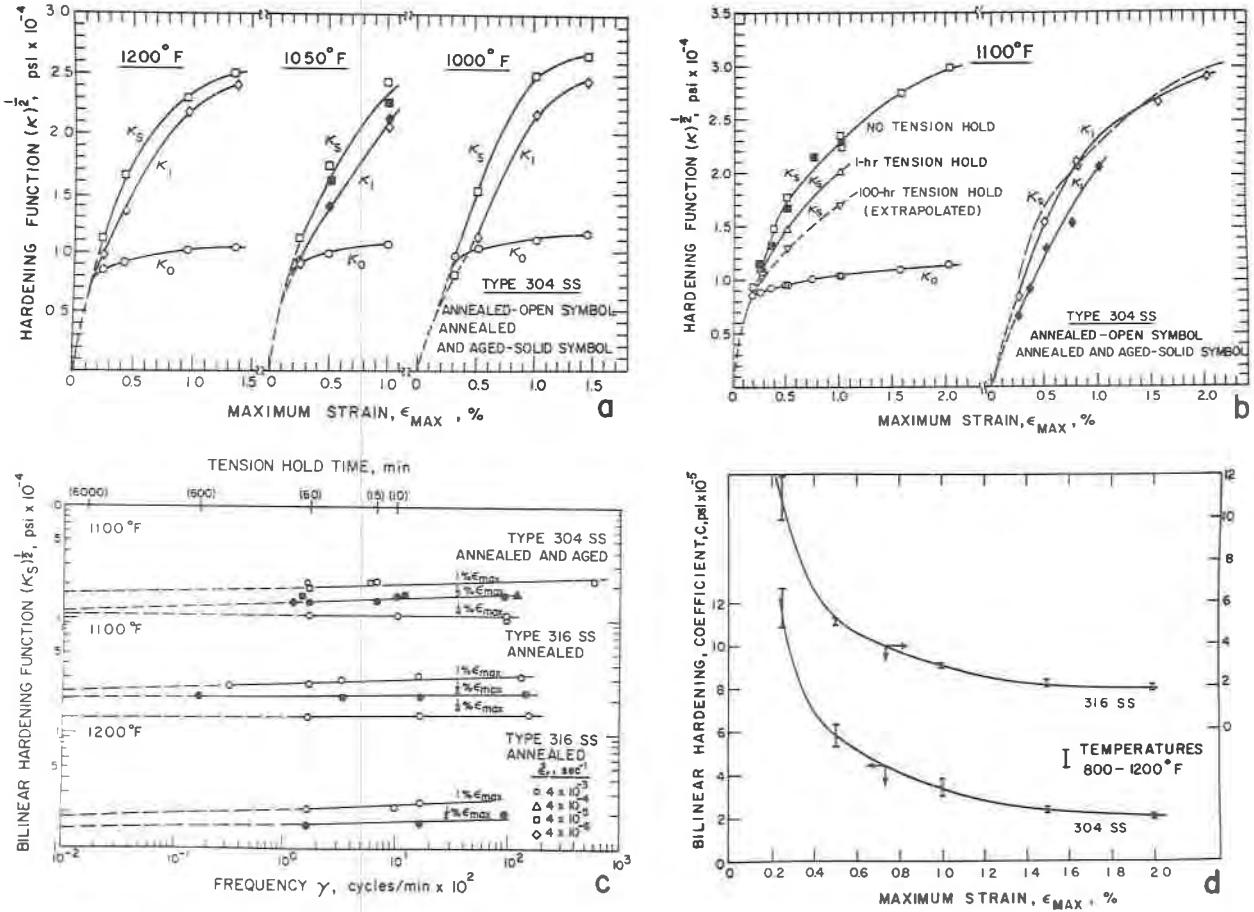


Fig. 3 Type 304 stainless steel. (a) and (b) Square root of hardening function κ vs maximum strain $\varepsilon_{max}$ at 1200, 1050 and 1000°F (a) and 1100°F (b). (c) Square root of hardening function κ vs equivalent frequency γ at 1100 and 1200°F (tension hold time at 4 x $10^{-3}$ $sec^{-1}$ ramp strain rate). (d) Bilinear hardening coefficient C vs maximum strain $\varepsilon_{max}$ from 800 to 1200°F.

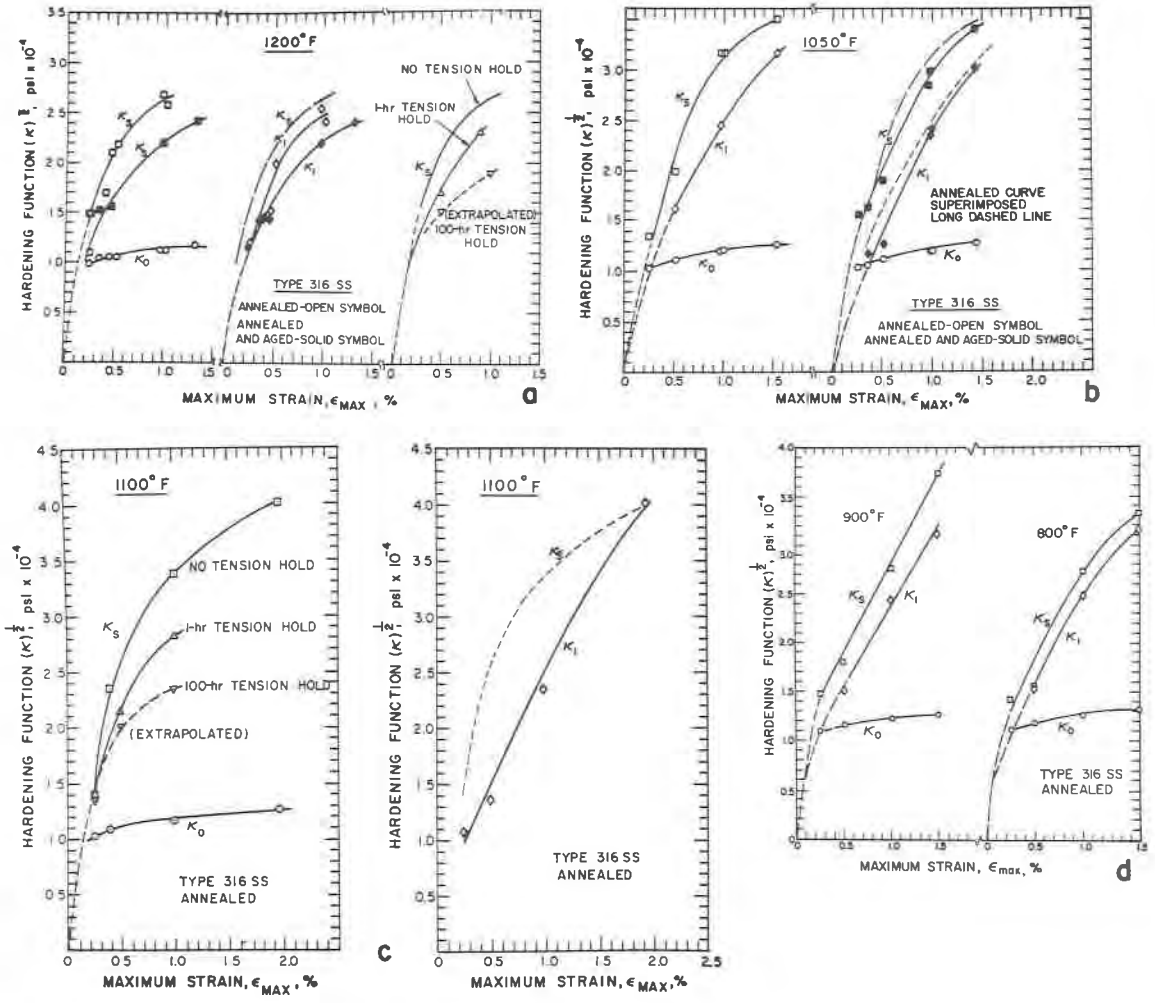


Fig. 4. Type 316 stainless steel. Square root of hardening function κ vs maximum strain $\epsilon_{max}$ at 1200°F (a), 1050°F (b), 1000°F (c), and 900 and 1000°F (d).